



## Research Publication Repository

<http://publications.wehi.edu.au/search/SearchPublications>

Author's accepted manuscript	Pearson JS, Giogha C, Muhlen S, Nachbur U, Pham CL, Zhang Y, Hildebrand JM, Oates CV, Lung TW, Ingle D, Dagley LF, Bankovacki A, Petrie EJ, Schroeder GN, Crepin VF, Frankel G, Masters SL, Vince J, Murphy JM, Sunde M, Webb AI, Silke J, Hartland EL. EspL is a bacterial cysteine protease effector that cleaves RHIM proteins to block necroptosis and inflammation. <i>Nature Microbiology</i> . 2017 2:16258
Final published version:	<a href="https://doi-org/10.1038/nmicrobiol.2016.258">https://doi-org/10.1038/nmicrobiol.2016.258</a>
Copyright:	© 2017 Macmillan Publishers Limited, part of Springer Nature. All Rights Reserved.

1 **EspL is a bacterial cysteine protease effector that cleaves RHIM proteins to block necroptosis**  
2 **and inflammation**

3

4 Jaclyn S. Pearson<sup>1\*</sup>, Cristina Giogha<sup>1\*</sup>, Sabrina Mühlen<sup>1<sup>∞</sup></sup>, Ueli Nachbur<sup>2,3</sup>, Chi L. L. Pham<sup>4</sup>, Ying  
5 Zhang<sup>1</sup>, Joanne M. Hildebrand<sup>2,3</sup>, Clare V. Oates<sup>1</sup>, Tania Wong Fok Lung<sup>1</sup>, Danielle Ingle<sup>1</sup>, Laura  
6 F. Dagley<sup>2,3</sup>, Aleksandra Bankovacki<sup>2,3</sup>, Emma J. Petrie<sup>2,3</sup>, Gunnar N. Schroeder<sup>5^</sup>, Valerie F.  
7 Crepin<sup>5</sup>, Gad Frankel<sup>5</sup>, Seth L. Masters<sup>2,3</sup>, James Vince<sup>2,3</sup>, James M. Murphy<sup>2,3</sup>, Margaret Sunde<sup>4</sup>,  
8 Andrew I. Webb<sup>2,3</sup>, John Silke<sup>2,3</sup> and Elizabeth L. Hartland<sup>1#</sup>

9 \*equal contribution

10

11 <sup>1</sup>Department of Microbiology and Immunology, University of Melbourne at the Peter Doherty  
12 Institute for Infection and Immunity, Melbourne 3000, Australia

13 <sup>2</sup>The Walter and Eliza Hall Institute of Medical Research, Parkville, Victoria 3052, Melbourne,  
14 Australia

15 <sup>3</sup>Department of Medical Biology, University of Melbourne, Victoria 3010, Australia

16 <sup>4</sup>Discipline of Pharmacology, School of Medical Sciences, University of Sydney, New South Wales  
17 2006, Australia

18 <sup>5</sup>MRC Centre for Molecular Bacteriology and Infection, Department of Life Sciences, Imperial  
19 College London, SW7 2AZ, UK

20

21 <sup>∞</sup> Current address: Department of Molecular Infection Biology, Helmholtz-Centre for Infection  
22 Research, 38124 Braunschweig, Germany

23 <sup>^</sup> Current address: Centre for Experimental Medicine, Queen's University Belfast, BT9 7BL, UK

24

25 <sup>#</sup>Correspondence: hartland@unimelb.edu.au

26

27 **Manuscript information:**

28 **Word count:** 1420

29 **Running title:** Type III effector EspL blocks necroptosis

30 **Keywords:** EPEC/necroptosis/RHIM/cysteine protease

31

32 Cell death signalling pathways contribute to tissue homeostasis and provide innate protection  
33 from infection. Adaptor proteins such as RIPK1, RIPK3, TRIF and ZBP1/DAI that contain  
34 receptor-interacting protein (RIP) homotypic interaction motifs (RHIM) play a key role in  
35 cell death and inflammatory signalling<sup>1-3</sup>. RHIM-dependent interactions help drive a caspase-  
36 independent form of cell death termed necroptosis<sup>4,5</sup>. Here we report that the bacterial  
37 pathogen enteropathogenic *Escherichia coli* (EPEC) uses the type III secretion system (T3SS)  
38 effector EspL to degrade the RHIM containing proteins, RIPK1, RIPK3, TRIF and  
39 ZBP1/DAI during infection. This required a previously unrecognised tripartite cysteine  
40 protease motif in EspL (Cys<sup>47</sup>, His<sup>131</sup>, Asp<sup>153</sup>) that cleaved within the RHIM of these proteins.  
41 Bacterial infection and/or ectopic expression of EspL led to rapid inactivation of RIPK1,  
42 RIPK3, TRIF and ZBP1/DAI and inhibition of TNF, LPS or poly(I:C)-induced necroptosis  
43 and inflammatory signalling. Furthermore, EPEC infection inhibited TNF-induced  
44 phosphorylation and plasma membrane localization of MLKL. *In vivo*, EspL cysteine  
45 protease activity contributed to persistent colonization of mice by the EPEC-like mouse  
46 pathogen *Citrobacter rodentium*. The activity of EspL defines a family of T3SS cysteine  
47 protease effectors found in a range of bacteria and reveals a mechanism by which  
48 gastrointestinal pathogens directly target RHIM-dependent inflammatory and necroptotic  
49 signalling pathways.

50

51 RHIM containing proteins, including RIPK1, RIPK3, TRIF and ZBP1/DAI, play essential roles in  
52 the regulation of inflammatory and cell death-signalling pathways<sup>5</sup>. RIPK1 is a key regulator of the  
53 NF- $\kappa$ B signalling pathway in response to TNF/TNFR1 stimulation, and may induce apoptosis  
54 through formation of a cytosolic complex containing TRADD/FADD and caspase-8<sup>6</sup>. However,  
55 upon inhibition of caspase-8 activity, RIPK1 binds RIPK3 through RHIM-RHIM interactions  
56 leading to phosphorylation of RIPK3 and the recruitment and phosphorylation of MLKL by

57 activated RIPK3<sup>7-11</sup>. Phosphorylated oligomeric MLKL translocates to the plasma membrane,  
58 which leads to the caspase independent form of cell death termed necroptosis<sup>12,13</sup>. Necroptosis may  
59 also result from TRIF or DAI/ZBP1 interactions with RIPK1 and RIPK3, which are also mediated  
60 by RHIM-RHIM interactions<sup>14,15</sup>. In addition, RIPK3 can promote NLRP3 inflammasome  
61 activation independently of necroptosis that is thought to be triggered by RHIM-RHIM amyloid  
62 formation<sup>16</sup>.

63

64 Infection of intestinal epithelial cells with the attaching and effacing enteropathogen, EPEC, leads  
65 to rapid inhibition of host inflammatory and apoptosis signalling pathways due to the activity of  
66 T3SS effectors<sup>17</sup>. While studying the effect of EPEC infection on assembly of the TNFR1 receptor  
67 complex, we observed that RIPK1 was rapidly degraded during wild type EPEC infection  
68 (E2348/69) but not during infection with the T3SS mutant (*ΔescN*) (Supplementary Figure 1a). By  
69 testing derivatives of EPEC lacking the genomic islands *PP4* alone (*ΔPP4*) or *PP4* and *IE6*  
70 (*ΔPP4/IE6*), we identified *IE6* and subsequently the gene encoding the effector EspL as essential  
71 for T3SS-dependent RIPK1 degradation (Fig. 1a; Supplementary Figure 1b). *espL* is located  
72 upstream of the T3SS effector genes, *nleB1* and *nleE*, which encode known inhibitors of apoptosis  
73 and NF-κB activation respectively (Fig. 1a)<sup>18-20</sup>. We confirmed that EspL was translocated by the  
74 T3SS using the TEM1 β-lactamase reporter<sup>21</sup> and that deletion of *espL* had no impact on actin  
75 accretion by EPEC, a measure of adherence and T3SS activity (Supplementary Figure 1c-e).

76

77 In mammalian cells, RIPK1 may be removed by K48-linked ubiquitylation and proteosomal  
78 degradation or by caspase-mediated cleavage<sup>22-24</sup>. However, neither caspase nor proteasome  
79 inhibitors, z-VAD-FMK (z-VAD) and MG132 respectively, prevented EspL-dependent loss of  
80 RIPK1 (Fig. 1b). Therefore, we speculated that EspL might mediate direct degradation of RIPK1.

81 Although amino acid sequence analysis failed to uncover any canonical protease motifs, alignment

82 of EspL with homologues identified by BLAST<sup>25</sup> from a range of bacterial pathogens revealed a  
83 putative conserved cysteine protease motif with the possible catalytic residues Cys<sup>47</sup>, His<sup>131</sup> and  
84 Asp<sup>153</sup> (Fig. 1c, d, 2a; Supplementary Figure 2). Despite lacking primary amino acid sequence  
85 similarity with known cysteine proteases, the secondary structure of EspL predicted by Phyre<sup>26</sup>  
86 showed N-terminal similarity to the CA clan of papain-like cysteine proteases, which includes the  
87 unrelated T3SS effector YopT from *Yersinia* spp. (Fig. 1c)<sup>27</sup>. Despite this, the broad spectrum  
88 cysteine protease inhibitors, antipain and Z-FA-FMK had no or only weak effect on EspL activity  
89 (Supplementary Figure 1f). Complementation of EPEC strain  $\Delta$ PP4/IE6 or the  $\Delta$ espL mutant with  
90 native EspL expressed *in trans* restored RIPK1 degradation. However, alanine substitution of Cys<sup>47</sup>,  
91 His<sup>131</sup> and Asp<sup>153</sup> but not Cys<sup>40</sup> abrogated EspL-induced RIPK1 degradation, confirming the crucial  
92 role of these amino acids in EspL activity (Fig. 1d).

93

94 To determine the specificity of EspL for RIPK1 degradation, we examined the effect of EPEC  
95 infection on human as well as murine RIP kinases by immunoblot. In addition to RIPK1,  
96 catalytically active EspL also induced loss of RIPK3, which shares a high degree of similarity with  
97 RIPK1<sup>28</sup> (Fig. 1d, Supplementary Figure 3a). Levels of RIPK2 were unaffected by EspL. Using an  
98 antibody generated to residues 385-650 of RIPK1, we detected a ~14 kDa cleavage product  
99 following ectopic expression of codon optimised Flag-EspL in HEK293T cells, suggesting that  
100 EspL removed the C-terminus of RIPK1 which encompasses the RHIM (Supplementary Figure 3b).  
101 To test the ability of EspL to cleave all mammalian RHIM containing proteins directly, we  
102 incubated purified recombinant EspL with the purified RHIM-containing regions of RIPK1, RIPK3,  
103 TRIF and ZBP1 and observed cleavage by catalytically active EspL for all RHIM proteins (Fig. 2b).  
104 Intact mass spectrometry and N-terminal sequencing of the cleavage products from RIPK3 and  
105 TRIF identified the cleavage site as QxGxx↓N (P5-P4-P3-P2-P1-P1') (Fig. 2b, c, Supplementary  
106 Figure 3c, d). Substitution of V<sup>448</sup>, Q<sup>449</sup>, I<sup>450</sup> and G<sup>451</sup> with alanine abrogated the ability of EspL to

107 cleave RIPK3 during EPEC infection suggesting that this conserved RHIM sequence was important  
108 for substrate recognition by EspL (Supplementary Figure 3e). EspL also possessed the ability to  
109 cleave the viral RHIM containing protein M45 from MCMV (Supplementary Figure 3f).

110

111 Given the observed cleavage of RIPK1 and RIPK3, we hypothesised that EspL would prevent  
112 RIPK1/RIPK3-dependent necroptosis. Mouse dermal fibroblasts (MDF) were used to create stable,  
113 doxycycline inducible cell lines expressing EspL or EspL<sub>C47S</sub>. Induction of catalytically active EspL  
114 was coincident with loss of RIPK1 and RIPK3 and this effect was reversible upon removal of  
115 induction (Supplementary Figure 4a, b). Cells expressing EspL were protected from necroptotic cell  
116 death, as measured by PI uptake, when induced by treatment with TNF, QVD or z-VAD (as caspase  
117 inhibitors) and the Smac-mimetic IAP antagonist, compound A (Cp.A) as an inhibitor of NF- $\kappa$ B  
118 activation<sup>29</sup>. These conditions are known to induce cell death by necroptosis<sup>13</sup>. This protection  
119 required EspL activity (Supplementary Figure 4c, 5a, b). EspL expression in MDF cells also  
120 prevented MLKL oligomerization and membrane translocation (Supplementary Figure 5c), two  
121 hallmarks of necroptosis<sup>13</sup>. During infection, EPEC blocked MLKL phosphorylation,  
122 oligomerization and membrane translocation and consequently necroptosis in HT-29 cells in an  
123 EspL dependent manner (Fig. 3, Supplementary Figure 6).

124

125 Apart from EspL, the T3SS effector NleB1 from EPEC can block TNF induced necroptosis by  
126 modifying a conserved arginine in the death domain of RIPK1 with *N*-acetyl glucosamine  
127 (GlcNAc)<sup>19</sup>. Consistent with partial redundancy in EspL and NleB1 function, only EPEC  
128 derivatives lacking both *espL* and *nleB1* ( $\Delta$ PP4/IE6 or  $\Delta$ espL/nleBE) were unable to inhibit TNF-  
129 induced necroptosis (Fig. 3b; Supplementary Figure 6). In addition, complementation of  $\Delta$ PP4/IE6  
130 with either active EspL or NleB but not NleE, restored EPEC-mediated inhibition of necroptosis

131 whereas inactive EspL (EspL<sub>C47S</sub>) or NleB1 (NleB1<sub>AAA</sub>)<sup>18,19</sup> did not (Fig. 3, Supplementary Figure  
132 6).

133

134 Consistent with loss of RIPK1, ectopic expression of EspL, but not inactive EspL, blocked TNF-  
135 induced expression of an NF-κB dependent luciferase reporter (Supplementary Figure 7a). In  
136 addition, EspL delivered by the T3SS in the EPEC mutant background *ΔPP4/IE6* resulted in  
137 reduced IL-8 production by infected HT-29 cells (Supplementary Figure 7b). EspL dependent loss  
138 of TRIF following EPEC infection or ectopic expression resulted in impaired interferon-β (*Inffβ*)  
139 expression and necroptosis induced by the TLR3 and TLR4 ligands, poly(I:C) and LPS,  
140 respectively (Fig. 4a, b, Supplementary Figure 7c). Using immortalised bone marrow derived  
141 macrophages (iBMDM), we observed that EspL blocked NLRP3/RIPK3-dependent caspase-1  
142 activation induced by treatment with Cp.A/QVD<sup>16</sup>, whereas activation of the canonical NLRP3  
143 inflammasome by nigericin was unaffected (Supplementary Figure 7d).

144

145 Although EspL possessed the ability to cleave all mammalian RHIM-containing proteins, a time  
146 course comparing RIPK1 and RIPK3 cleavage suggested that RIPK1 was the preferred target  
147 during EPEC infection (Supplementary Figure 8a). In addition, cleavage likely occurred before  
148 amyloid formation as RHIM fibrils were only inefficiently cleaved by EspL compared to the  
149 monomeric proteins (Supplementary Figure 8b, c). Amyloid fibrils form the signalling scaffold of  
150 the necrosome and arise from RHIM-RHIM interactions between RIPK1 and RIPK3<sup>4</sup>.

151

152 The targeted inhibition of necroptosis and RHIM-dependent inflammatory signalling by EspL  
153 during EPEC infection suggested that the activity of EspL might aid mucosal immune evasion. Here  
154 we assessed the ability of derivatives of the EPEC-like mouse pathogen, *C. rodentium* to colonise  
155 wild type C57BL/6 mice. *C. rodentium* is a murine attaching and effacing pathogen that carries all

156 the conserved T3SS effector genes present in EPEC, including *espL*. We confirmed that EspL from  
157 *C. rodentium* (CREspL) cleaved RIPK1, whereas inactive CREspL<sub>C42S</sub> did not (Fig. 4c). In wild  
158 type C57BL/6 mice, we observed that an *espL* mutant of *C. rodentium* was attenuated for intestinal  
159 colonization in the resolving phase of infection suggesting that EspL promoted bacterial persistence  
160 in the gut, similar to previous findings<sup>30</sup> (Supplementary Figure 9). Complementation of the *espL*  
161 mutant with *espL* but not *espL*<sub>C47S</sub> restored intestinal colonization by *C. rodentium* (Fig. 4d)  
162 suggesting that the cysteine protease activity of EspL was critical to its virulence function. Given  
163 the semi-redundant activities of EspL and NleB1 that we observed in the inhibition of necroptosis,  
164 and the fact that *nleB* mutants of *C. rodentium* also exhibit a colonization defect<sup>18,19</sup>, further work  
165 should examine the relative contribution of each effector in vivo using an *espL/nleB* double mutant  
166 of *C. rodentium* complemented with active and inactive forms of NleB and EspL.

167

168 Here we have defined EspL from EPEC as the prototypic member of a family of T3SS cysteine  
169 protease effectors and identified the targets of EspL as host RHIM-containing proteins. EspL  
170 inactivated inflammatory, inflammasome and necroptotic signalling by cleaving within the RHIM,  
171 thereby disrupting a range of host mucosal defence pathways. EspL adds to the arsenal of bacterial  
172 T3SS effectors that subvert host cell signalling and the presence of, as yet uncharacterised, EspL  
173 homologues in a broad range of bacterial pathogens suggests that this family of cysteine protease  
174 effectors constitutes a widespread virulence mechanism.

175

## 176 **Acknowledgments**

177 We gratefully acknowledge Edward Mocarski (Emory University) for the gift of Flag-ZBP1/DAI  
178 and Flag-M45 and Gabrielle Belz (Walter and Eliza Hall Institute) for animal ethics assistance. We  
179 thank Sam Young (Walter and Eliza Hall Institute) for technical assistance. This work was  
180 supported by the Australian National Health and Medical Research Council (Program Grant



181 ID606788 to ELH, Project Grants APP1057888 to JS and APP1051210 to JV and APP1057905 to  
182 JMM and JS; Fellowships APP1090108 to JSP, APP1052598 to JV and APP1105754 to JMM) and  
183 the Australian Research Council (Future Fellowship FT130100166 to UN, Discovery Project  
184 DP150104227 to MS). CG and DI were supported by Australian Postgraduate Awards. TW was  
185 supported by a University of Melbourne International Research Scholarship (MIRS). GNS is funded  
186 by the Medical Research Council, UK. This work was made possible through Victorian State  
187 Government Operational Infrastructure Support and Australian Government NHMRC IRIISS. The  
188 authors declare no financial interests related to this work.

189

190 **Author contributions.** J.S.P., C.G., S. M., U. N, C.L.L.P., Y.Z., J.M.H., T.W., D. I., A.B., E. J. P.  
191 J.V. and M.S. designed and performed the experiments. S.L.M., J.M., G.N.S., C.V.O., V.F.C. and  
192 G.F contributed reagents and expertise. L.F.D. and A.I.W. performed mass spectrometry analyses.  
193 J.S.P. C. G, J.S. and E.L.H. designed the experiments and wrote the manuscript.

194

195 **METHODS**

196 **Bacterial strains, plasmids, cell lines and growth conditions**

197 The bacterial strains, plasmids and oligonucleotide primers used in this study are listed in  
198 Table S1. Bacteria were grown at 37 °C in Luria-Bertani (LB) medium, Dulbecco's Modified  
199 Eagle's medium (DMEM) with GlutaMAX (Gibco, NY), or Roswell Park Memorial Institute  
200 medium (RPMI) with GlutaMAX (Gibco) where indicated and supplemented with ampicillin (100  
201 µg/mL), kanamycin (100 µg/mL), nalidixic acid (50 µg/mL) or chloramphenicol (25 µg/mL) where  
202 necessary.

203 Mouse dermal fibroblasts (MDFs) were isolated from the dermis of adult mice and  
204 immortalised with SV40 large T antigen<sup>31</sup>. Bone marrow derived macrophages from C57BL/6  
205 mice were immortalized to generate a macrophage cell line (iBMDM) with CreJ2 virus as described  
206 previously<sup>32</sup>. All other cell lines were sourced from and authenticated by either the ATCC Global  
207 Bioresource Centre, or the ECACC via Sigma-Aldrich. HeLa cells, HEK293T cells, Caco-2 cells,  
208 iBMDMs, MDFs and MEFs were grown in DMEM GlutaMax (Gibco) supplemented with 10%  
209 FCS (Sigma) at 37 °C with 5% CO<sub>2</sub>. HT-29 cells were grown in Roswell Park Memorial Institute  
210 medium (RPMI) GlutaMAX (Gibco) with 10% FCS (Sigma) at 37 °C with 5% CO<sub>2</sub>.

211 **Construction of EspL expression vectors**

212 For expression in bacteria, the *espL* gene was amplified from EPEC E2348/69 genomic  
213 DNA by PCR using the primer pair EspL<sub>F</sub>/EspL<sub>R</sub> for cloning into pTrc99A. PCR amplification  
214 consisted of an initial denaturation step at 95 °C for 10 min, followed by 30 cycles of 94 °C for 44  
215 sec, 55 °C for 45 sec and 70 °C for 2 min followed by a final elongation step of 70°C for 10 min.  
216 The PCR product was digested with KpnI and EcoRI and ligated into pTrc99A to produce pEspL.

217 For expression in mammalian cells, the gene encoding EspL from either EPEC E2348/69 or  
218 *C. rodentium* ICC169 was codon-optimised (DNA2.0), amplified using the primer pair  
219 EspL<sub>COF</sub>/EspL<sub>COR</sub> or EspL<sub>CRCOF</sub>/EspL<sub>CRCOR</sub> and ligated into KpnI/BamHI digested p3XFlag-MyC-

220 CMV-24 to generate N-terminal 3xFlag fusions of EspL (pFlag-EspL or pFlag-CREspL). For  
221 construction of the lentiviral plasmid to generate stable inducible cell lines, codon optimised Flag-  
222 EspL was amplified from pFlag-EspL and ligated into pF TRE3G PGK puro<sup>10,29</sup> using  
223 BamHI/XbaI.

224 Genes encoding residues 2-549 of EPEC E2348/68 EspL and EspL<sub>C47S</sub> were amplified by  
225 PCR using pEspL and pEspL<sub>C47S</sub> as template DNA respectively, using the primer pair  
226 EspL<sub>GEXF</sub>/EspL<sub>GEXR</sub>. PCR products were digested with BamHI and NotI and ligated into the vector  
227 pGEX-2T-TEV, as previously described<sup>33</sup> to enable bacterial expression with an in-frame N-  
228 terminal GST fusion. Insert sequences were verified by Sanger sequencing (Micromon, Monash  
229 University, Australia).

### 230 **Site-directed mutagenesis**

231 Site-directed mutants were generated using the Stratagene QuikChange II Site-Directed  
232 Mutagenesis Kit according to manufacturer's protocol. pEspL<sub>C40S</sub>, pEspL<sub>C47S</sub>, pEspL<sub>H131A</sub>,  
233 pEspL<sub>D153A</sub> were generated using pEspL as template DNA and primer pairs EspL<sub>(C40S)F</sub>/EspL<sub>(C40S)R</sub>,  
234 EspL<sub>(C47S)F</sub>/EspL<sub>(C47S)R</sub>, EspL<sub>(H131A)F</sub>/EspL<sub>(H131A)R</sub> and EspL<sub>(D153A)F</sub>/EspL<sub>(D153A)R</sub> respectively. pFlag-  
235 EspL<sub>C40S</sub>, pFlag-EspL<sub>C47S</sub>, pFlag-EspL<sub>H131A</sub>, pFlag-EspL<sub>D153A</sub> were generated using pFlag-EspL as  
236 template DNA and primer pairs EspL<sub>(C40S)COF</sub>/EspL<sub>(C40S)COR</sub>, EspL<sub>(C47S)COF</sub>/EspL<sub>(C47S)COR</sub>,  
237 EspL<sub>(H131A)COF</sub>/EspL<sub>(H131A)COR</sub> and EspL<sub>(D153A)COF</sub>/EspL<sub>(D153A)COR</sub> respectively. pF TREG-Flag-  
238 EspL<sub>C47S</sub> was generated using pF TREG-Flag-EspL as template DNA and primer pair  
239 EspL<sub>(C47S)COF</sub>/EspL<sub>(C47S)COR</sub>. pFlag-CREspL<sub>C42S</sub> was generated using pFlag-CREspL as template  
240 DNA and primer pair EspL<sub>C42S(CO)F</sub>/EspL<sub>C42S(CO)R</sub>. pGEX-EspL<sub>C47S</sub> was generated by PCR-  
241 amplification of a cDNA encoding EPEC E2348/69 EspL<sub>C47S</sub> (pTrc-EspL<sub>C47S</sub>) using primers  
242 EspL<sub>GEXF</sub>/EspL<sub>GEXR</sub> bearing restriction sites (5' BamHI, 3' NotI), followed by restriction digest and  
243 ligation into the vector, pGEX-2T-TEV (pGEX-EspL<sub>C47S</sub>). pGFP-mRIPK3<sub>AAAA</sub> was generated  
244 using pGFP-mRIPK3 as template DNA and primer pair mRIPK3<sub>AAAA-F</sub>/mRIPK3<sub>AAAA-R</sub>.

## 245 **Purification of GST-EspL**

246 600 mL Super broth cultures containing 100 µg/mL ampicillin were inoculated with *E. coli*  
247 BL21 Codon Plus transformed with GST-EspL or GST-EspL<sub>C47S</sub> expression constructs and cultured  
248 at 37 °C with shaking to OD<sub>600</sub> of 0.6-0.8. Cultures were then cooled to 18 °C, protein expression  
249 induced by addition of 1 mM IPTG with continued shaking and incubation at 18 °C overnight. Cell  
250 pellets were resuspended in lysis buffer (200 mM NaCl, 20 mM HEPES pH 7.5, 5% w/v glycerol,  
251 0.5 mM TCEP), before lysis by sonication, elimination of debris by centrifugation at 45000 g, 0.45  
252 µm filtration of the lysate and incubation with glutathione agarose (UBP Bio) at 4 °C with agitation  
253 for 1-2 h. Beads were collected and washed with lysis buffer before incubation with 200 µg TEV  
254 protease at 20 °C for 2 h on rollers. Supernatant containing cleaved EspL or EspL<sub>C47S</sub> was  
255 concentrated by centrifugal ultrafiltration and loaded on to Superdex S200 gel filtration column pre-  
256 equilibrated with gel filtration buffer (200 mM NaCl, 20 mM HEPES pH 7.5, 5% v/v glycerol).  
257 Fractions containing purified EspL or EspL<sub>C47S</sub>, as assessed by SDS-PAGE, were pooled,  
258 concentrated by centrifugal ultrafiltration to 5 mg/mL, aliquoted, snap frozen in liquid nitrogen and  
259 stored at -80 °C until required.

## 260 **RHIM domain protein constructs, expression and purification**

261 Synthetic genes encoding RHIM-containing regions of human RIPK1 (Q13546; residues  
262 497-583), human RIPK3 (Q9Y572; residues 387-518), human DAI/ZBP1 (Q9H171; residues 170-  
263 429), human TRIF (Q8IUC6; residues 601-712) with flanking BamHI and EcoRI restriction sites  
264 were purchased from Genscript, digested with these restriction enzymes, purified by agarose gel  
265 electrophoresis and ligated individually into the pHUE vector cut with the same two restriction  
266 enzymes<sup>34</sup>. All expressed fusion proteins therefore consist of His6-ubiquitin-RHIM region.  
267 Successful cloning was confirmed by sequencing at AGRF (Westmead Institute) Sydney. Proteins  
268 were expressed in BL21(DE3) grown at 37 °C to an OD<sub>600</sub> of 0.6-0.8, and induced with 0.5 mM  
269 IPTG for 3 h. Cell pellets were lysed in 6M GuHCl, 100 mM NaH<sub>2</sub>PO<sub>4</sub>, 20 mM Tris.Cl, 5 mM β

270 mercaptoethanol, pH 8.0, and soluble material further purified on Ni-NTA agarose under denaturing  
271 conditions, with exchange into 8 M urea, 100 mM NaH<sub>2</sub>PO<sub>4</sub>, 20 mM Tris, 5 mM β mercaptoethanol  
272 at pH 6.0 for washing and pH 4.0 for elution from the Ni-NTA agarose.

273 **Generation of stable inducible cell lines in mouse dermal fibroblasts (MDF) and immortalized**  
274 **bone marrow derived macrophages (iBMDM)**

275 HEK293T cells were seeded at 2 x 10<sup>5</sup> cells per 10 cm culture dishes and 24 h later were co-  
276 transfected with 10 μg of either pF TRE3G-Flag-EspL or pF TRE3G-Flag-EspL<sub>C47S</sub> along with the  
277 helper plasmids pMDL-RRE, pRSV-REV and pVSV-g (5, 2.5 and 3 μg, respectively) using  
278 Effectine Transfection Reagent (QIAGEN) for a further 24 h. Culture media was then changed and  
279 the cells were incubated for a further 48 h for virus production. Polybrene (5 μg/mL) (Sigma) was  
280 added to the cell culture dishes and the virus-containing supernatant was collected and passed  
281 through a 0.45 μm filter. Virus-containing supernatant was added to either MDF monolayers or  
282 iBMDM monolayers and incubated at 37 °C with 5% CO<sub>2</sub> for 24 h. Infected cells were selected for  
283 using increasing concentrations of up to 5 μg/mL of puromycin (Sigma) for at least one week.  
284 Expression of Flag-EspL or Flag-EspL<sub>C47S</sub> in either MDFs or iBMDMs was tested by adding 20  
285 ng/mL doxycycline at varying time points followed by immunoblot using anti-Flag antibodies.

286 **Construction of *Citrobacter rodentium* *espL* mutant**

287 A 325 bp upstream region of *espL* was amplified using primer pair Up-EspL-Fw/BamHI-  
288 Up-EspL-Rv, and a 500 bp downstream region of *espL* was amplified using primer pair BamHI-  
289 Down-EspL-Fw/Down-EspL-Rv. Both fragments were then digested with BamHI, ligated together,  
290 and cloned into pGEMT. The non-polar *aphT* cassette<sup>35</sup> was then inserted into the BamHI site  
291 between the two fragments and the orientation of the *aphT* cassette ascertained by PCR. This  
292 construct was then amplified using the primer pair Up-EspL-Fw/Down-EspL-Rv. The PCR  
293 products were electroporated into ICC169 containing pKD46 encoding lambda red recombinase<sup>36</sup>.

294 Transformants were selected on kanamycin agar plates and *espL* deletion confirmed by PCR  
295 (Check-EspL-UP-Fw /Down-EspL-Rv) and DNA sequencing.

### 296 ***cis* complementation of the *Citrobacter rodentium espL* mutant**

297 The *Citrobacter rodentium espL* mutant was *cis* complemented with either WT *espL* or  
298 *espL<sub>C42S</sub>* using the transgene insertion method previously described<sup>37</sup>. Briefly, the *espL* gene with  
299 its native promoter was amplified from *C. rodentium* ICC169 genomic DNA template by PCR  
300 using primers EspL<sub>CRF1</sub>/EspL<sub>CRR1</sub>, and then ligated into the XmaI/XhoI restriction sites of the  
301 pGRG36 vector. The pGRG36-EspL<sub>C42S</sub> construct was generated by site-directed mutagenesis. The  
302 pGRG36-EspL construct was used as template DNA and amplified by PCR using primers  
303 EspL<sub>C42SF</sub>/EspL<sub>C42SR</sub>. The resulting plasmid was digested with DpnI at 37 °C overnight before  
304 transformation into the appropriate *E. coli* strain.

305 The pGRG36-EspL and pGRG36-EspL<sub>C42S</sub> constructs were confirmed by PCR using  
306 primers Tn7<sub>F</sub>/Tn7<sub>R</sub>, then electroporated into electrocompetent *C. rodentium espL* mutant cells and  
307 selected for using 100 ug/mL ampicillin and incubated at 30 °C overnight. Transformants were  
308 streaked out once, then grown overnight in LB without antibiotics at 30 °C. Dilutions were prepared  
309 and plated on LB and grown overnight at 42 °C. Transposition of the Tn7:*espL/espL<sub>C42S</sub>* into the  
310 *attTn7* insertion site in the *C. rodentium espL* mutant chromosome was confirmed by the absence of  
311 the ampicillin resistance marker and PCR using primers CRseq<sub>F</sub>/CRseq<sub>R</sub>.

### 312 **Construction of EPEC single and triple deletion mutants**

313 To construct the EPEC E2348/69 *espL* deletion mutant strain, 342-bp and 331-bp fragments  
314 were amplified from 5' and 3' flanking sites of *espL* using oligonucleotides EspL<sub>5'F</sub>/ EspL<sub>5'R</sub> and  
315 EspL<sub>3'F</sub>/ EspL<sub>3'R</sub>. The plasmid pKD4 was used as template DNA to amplify the kanamycin cassette  
316 using oligonucleotides pKD3-4<sub>F</sub> and pKD3-4<sub>R</sub>. Overlapping PCR was used to assemble the *espL*  
317 flanking regions with the kanamycin cassette construct using oligonucleotides EspL<sub>5'F</sub> and EspL<sub>3'R</sub>.  
318 Lambda red mediated recombination<sup>36</sup> was used to replace the wild type allele with the kanamycin

319 resistance cassette. The cassette was electroporated into wild-type EPEC E2348/69 and positive  
320 clones were selected for on LB agar with 25 µg/mL kanamycin. To construct the EPEC E2348/69  
321 *espLnleBE* deletion mutant, a 368-bp fragment was amplified from 5' flanking site of *nleB* using  
322 oligonucleotides NleB<sub>5'F</sub>/ NleB<sub>5'R</sub> and 550-bp fragment was amplified from 3' flanking site of *nleE*  
323 using oligonucleotides NleE<sub>3'F</sub>/ NleE<sub>3'R</sub>. The plasmid pKD3 was used as template DNA to amplify  
324 the chloramphenicol cassette using oligonucleotides pKD3-4<sub>F</sub> and pKD3-4<sub>R</sub>. Overlapping PCR was  
325 used to assemble the *nleB* and *nleE* flanking regions with the chloramphenicol cassette construct  
326 using oligonucleotides NleB<sub>5'F</sub> and NleE<sub>3'R</sub>. Lambda red mediated recombination<sup>36</sup> was used to  
327 replace the wild type allele with the chloramphenicol resistance cassette. The cassette was  
328 electroporated into EPEC E2348/69 *espL* mutant cells and positive clones were selected for on LB  
329 agar with 5 µg/mL chloramphenicol. Deletions were confirmed by PCR with a combination of  
330 primers from outside and inside the altered region. Attachment and pedestal formation by parental  
331 and mutant strains were confirmed using fluorescence actin staining.

### 332 **EPEC infection**

333 Cell lines of HeLa, Caco-2, MDF and HT-29 cells are maintained in our laboratory and  
334 regularly tested for mycoplasma contamination. Two days prior to infection HeLa, Caco-2, MDF or  
335 HT-29 cell monolayers were seeded into 24 well tissue culture trays. One day prior to infection  
336 derivatives of EPEC were inoculated into LB broth and grown with shaking at 37 °C overnight. On  
337 the day of infection, overnight cultures of EPEC were sub-cultured 1:75 in DMEM GlutaMAX  
338 (Gibco) or RPMI GlutaMAX (Gibco) and grown statically for 3 h at 37 °C with 5% CO<sub>2</sub>. Where  
339 necessary, cells were induced with 1 mM isopropyl-B-D-thiogalactopyranoside IPTG (Sigma) 30  
340 min prior to infection. Cells were washed twice with PBS and infected with EPEC grown to an  
341 OD<sub>600nm</sub> of 0.03 for 1-3 h (depending on the experiment). When required, the inhibitors MG132  
342 (Sigma) (10 µM), antipain (Sigma) (10, 20 or 40 µg/mL), z-VAD-FMK (Abcam) (25 µM), or z-FA-

343 FMK (Abcam) (10, 20 or 40  $\mu$ M) were added to the cells 1 hr prior to infection and kept on for the  
344 duration of the infection.

#### 345 **Transfection**

346 All transfections were performed in HEK293T cells using Fugene® 6 (Promega)  
347 transfection reagent. Cells were seeded into 24 well tissue culture trays and transfected 24 h later  
348 with 1 $\mu$ g DNA for a period of ~18 h.

#### 349 **Fluorescent actin stain**

350 HeLa cells were seeded on coverslips and infected as previously described. After infection,  
351 cells were washed with PBS, fixed in 4 %PFA in PBS for 30 min and permeabilised in 1% Triton  
352 X-100 for another 30 min. Cells were then washed twice with PBS and stained with 4',6-diamidino-  
353 2-phenylindole (DAPI, Invitrogen) at 0.5 mg/mL and Phalloidin-Tetramethylrhodamine B  
354 isothiocyanate (Sigma) in 3% BSA/PBS for 30 min. Coverslips were mounted onto microscope  
355 slides with Prolong Gold anti-fade reagent (Invitrogen). Images were acquired using a Zeiss  
356 confocal laser scanning microscope with a 1003/EC Epiplan-Apochromat oil immersion objective.

#### 357 **Immunoblot analysis**

358 For immunoblot analysis following EPEC infection, transfection or induction of stable cell  
359 lines, cells were collected and lysed in cold lysis buffer (1% Triton X-100, 50 mM Tris-HCl, pH  
360 7.4, 1 mM EDTA, 150 mM NaCl) with Complete Protease Inhibitor (Roche), 2 mM Na<sub>3</sub>VO<sub>4</sub>, 10  
361 mM NaF, 1 mM PMSF and incubated on ice for 10 min to complete lysis. Samples were then  
362 pelleted at 4 °C by centrifugation and the supernatants added to 4×Bolt® LDS Sample Buffer  
363 (Thermo Fisher), heated to 70 °C for 10 min and resolved on Bolt® 4-12% Bis-Tris Plus Gels  
364 (Thermo Fisher) by PAGE. Proteins were transferred to nitrocellulose membranes using an iBlot2  
365 Gel Transfer Device (Thermo Fisher) and probed with one of the following primary antibodies:  
366 mouse monoclonal anti-RIPK1 (38/RIP) (BD Transduction Laboratories), mouse monoclonal anti-  
367 RIPK2/RICK (25/RIG-G) (BD Transduction Laboratories), rabbit polyclonal anti-RIPK3 (Abcam)



368 (for HT-29 cells), rabbit polyclonal anti-RIPK3 (ProSci) (for MDF cells) or rabbit polyclonal anti-  
369 TRIF (Cell Signaling), mouse monoclonal anti-Flag M2-HRP (Sigma), mouse monoclonal anti-  
370 GFP (7.1 and 13.1) (Roche), mouse monoclonal anti- $\beta$ -actin (AC-15) (Sigma), mouse monoclonal  
371 anti-TRADD (7G8) (Cell Signaling), rabbit polyclonal anti-TRAF2 (Cell Signaling), monoclonal  
372 rat anti-mouse MLKL (WEHI-3H1) (WEHI, made in-house), mouse monoclonal anti-TEM1  $\beta$ -  
373 lactamase (8A5.A10) (QED Bioscience) diluted in TBS with 5% BSA (Sigma) and 0.1% Tween  
374 (Sigma). Proteins were detected using anti-rabbit or anti-mouse IgG secondary antibodies  
375 conjugated to horseradish peroxidase (PerkinElmer) diluted in TBS with 5% BSA (Roche) and  
376 0.1% Tween (Sigma) and developed with enhanced chemiluminescence (ECL) western blotting  
377 reagent (Amersham). Images were visualised using an MFChemisBis imaging station (DNR, Israel).  
378 At least three biological replicates were performed for all experiments.

#### 379 **Cell viability assays (MTT and propidium iodide staining)**

380 For analysis of cell viability using MTT assays, immortalised mouse bone marrow-derived  
381 macrophages (iBMDM) stably expressing either EspL or EspL<sub>C47S</sub> were seeded into 24 well tissue  
382 culture plates (Corning) for 18-24 h before being left untreated or treated with 20 ng/mL of LPS (*E.*  
383 *coli* 0111:B4) (Sigma) or 50  $\mu$ g/mL Poly I:C (for iBMDMs) (Sigma) or 10  $\mu$ g/mL high molecular  
384 weight Poly I:C (InvivoGen, CA, USA) and 10  $\mu$ M z-VAD-FMK (Abcam) for a further 18 h. The  
385 cells were washed once with PBS and replaced with DMEM containing 0.1  $\mu$ g/mL 3-(4,5-  
386 Dimethylthiazol-2-yl)-2,5- diphenyltetrazolium bromide (MTT) (Sigma) for 1 h, after which the  
387 medium was removed and 100  $\mu$ L of dimethyl-sulfoxide (DMSO; Sigma) was added to each well.  
388 After thorough mixing on an orbital shaker for 1 min, the absorbance at 540 nm for each well was  
389 obtained using a CLARIOstar microplate reader (BMG Labtech, Germany). Results were obtained  
390 from at least 3 independent experiments.

391 For analysis of cell viability by propidium iodide (PI) staining of HT-29 monolayers, cells  
392 were seeded into 24 well tissue culture plates with sterile glass coverslips and 48 h later were

393 infected with EPEC derivatives as previously mentioned for 2.5 h followed by 4 h incubation in  
394 media supplemented with 50 µg/mL gentamicin and 20 ng/mL TNF (Calbiochem), 500 nM  
395 compound A (Cp. A, Tetralogic), 25 µM z-VAD-FMK (Abcam). PI (50 µg/mL) (Sigma) was added  
396 for the final 15 min of treatment. Cells were then fixed in 3.7% (wt/vol) formaldehyde (Sigma) in  
397 PBS for 10 min and permeabilised with 0.2% Triton (Sigma) for 4 min. 4', 6-diamidino-2-  
398 phenylindole (DAPI; Invitrogen) was applied at 0.5 µg/mL in PBS for 10 min. Cells were washed  
399 with PBS three times and coverslips were mounted onto microscope slides with Prolong Gold anti-  
400 fade reagent (Invitrogen). Images were acquired using a Zeiss confocal laser-scanning microscope  
401 with a 100x/EC Epiplan-Apochromat oil immersion objective. Duplicate coverslips were blinded  
402 for counting of PI positive cells, and results were obtained from at least 3 independent experiments.

403 For analysis of cell viability by PI staining and confocal microscopy in MDF cells, EspL  
404 and EspL<sub>C47S</sub> expressing lines were induced with 20 ng/mL doxycycline for 2 h followed by 4 h  
405 incubation in media supplemented with 20 ng/mL TNF (Calbiochem), 500 nM Cp. A (Tetralogic),  
406 25 µM z-VAD-FMK (Abcam). PI, DAPI staining and confocal microscopy were carried out as  
407 described above. Duplicate coverslips were blinded for counting of PI positive cells, and results  
408 were obtained from at least 3 independent experiments.

409 For analysis of cell viability by PI staining and flow cytometry, MDF-EspL and MDF-  
410 EspL<sub>C47S</sub>, cell lines were induced with 10 ng/mL doxycycline for 1 h followed by 24 h incubation in  
411 media supplemented with 100 ng/mL hTNF-Fc produced in house (WEHI), 500 nM Cp. A  
412 (Tetralogic), 50 µM QVD-OPH (Abcam). Cell death was assessed with PI staining (1 µg/mL) and  
413 quantified using a BD FACSCalibur flow cytometer. Data was analysed using the WEASEL Flow  
414 Cytometry Software.

#### 415 **Monitoring MLKL complex formation using BN-PAGE**

416 For MDF cells, 5 x 10<sup>5</sup> cells (wild type, stably expressing inducible Flag-EspL or Flag-  
417 EspL<sub>C47S</sub>) were used to seed each well of a 6 well tissue culture plate and allowed to attach

418 overnight. Cells were stimulated with 0.5 µg/mL doxycycline for 2 h to induce Flag-EspL  
419 expression prior to the addition of 100 ng/mL hTNF-Fc produced in house (WEHI), 500 nM Cp. A  
420 (Tetralogic), 25 µM z-VAD-FMK (Abcam) for a further 4 h to induce necroptosis. For HT29 cells,  
421  $5 \times 10^5$  cells were plated in each well of a six well plate and allowed to attach for 48 h. Cells were  
422 infected with derivatives of EPEC E2348/69 for 2.5 h followed by stimulation with 20 ng/mL TNF  
423 (Calbiochem), 500 nM Cp. A (Tetralogic), 25 µM z-VAD-FMK (Abcam) for a further 5 h to induce  
424 necroptosis. Cells were harvested by scraping and permeabilised in MELB buffer (20 mM HEPES  
425 (pH 7.5), 100 mM KCl, 2.5 mM MgCl<sub>2</sub>, 100 mM sucrose, 0.025% digitonin (BIOSYNTH, Staad,  
426 Switzerland) 2 µM N-ethyl maleimide, Complete Protease Inhibitor (Roche) and PhosSTOP  
427 phosphatase inhibitor cocktail (Roche)). Cytosolic and crude membrane fractions were separated by  
428 centrifugation and the crude membrane fraction further solubilized in MELB buffer containing 1%  
429 digitonin and clarified by centrifugation. Digitonin was added to the cytosolic fraction (final 1%  
430 w/v) and fractions were resolved on a 4-16% Bis-Tris Native PAGE gels (Thermo Fisher),  
431 transferred to PVDF and probed for rabbit anti-human phospho-MLKL (Abcam), monoclonal rat  
432 anti-mouse MLKL (WEHI-3H1) (WEHI, made in house), rabbit polyclonal anti-VDAC1  
433 (Millipore) and rabbit polyclonal anti-GAPDH (Cell Signaling).

#### 434 **Inflammasome activation**

435 iBMDMs (WT, EspL or EspL<sub>C47S</sub>) were seeded in 12 well tissue culture treated plates and  
436 treated with 50 ng/mL ultra-pure LPS (Invivogen) for 2 h then 1 µg/mL doxycycline (Sigma) added  
437 for an additional 2 h. Cells were subsequently stimulated with 1 µM Cp.A (Tetralogic  
438 pharmaceuticals) and/or 15 µM QVD-Oph (RnD Systems) for 6 h or 10 µM Nigericin (Sigma) for 1  
439 h. Cell supernatants and lysates were analysed by western blot. Primary antibodies used were  
440 mouse monoclonal anti-Flag M2-HRP (Sigma), mouse monoclonal caspase-1 (casper-1)  
441 (Adipogen), mouse monoclonal anti-RIPK1 (38/RIP) (BD Transduction), rabbit polyclonal RIPK3

442 (Axxora; PSC-2283-C100) and mouse monoclonal anti- $\beta$ -actin (AC-15) (Sigma). All antibody  
443 dilutions were performed in 5% skim milk/0.1% PBS Tween.

#### 444 **IL-8 secretion assay**

445 For analysis of IL-8 secretion, HT-29 cell monolayers were infected for 3 h before being  
446 incubated for 8-12 h in media supplemented with 50  $\mu$ g/mL gentamicin with or without 20 ng/mL  
447 TNF (Calbiochem, EMD4Biosciences, USA). Following this, the HT-29 cell supernatant was  
448 collected and either used immediately or stored at -20  $^{\circ}$ C for subsequent analysis of IL-8 secretion.  
449 IL-8 secretion was measured using the Human IL-8 ELISA MAX Deluxe Set (Biolegend, CA,  
450 USA) according to the manufacturer's instructions.

#### 451 **qRT-PCR**

452 Samples for qRT-PCR experiments were DNase treated using Ambion TURBO DNA-free  
453 kit and cDNA synthesis was completed using the iScript<sup>TM</sup> cDNA synthesis kit (Bio-Rad). qRT-  
454 PCR was performed using SsoAdvanced<sup>TM</sup> Universal SYBR<sup>®</sup> Green Supermix (Bio-Rad) according  
455 to manufacturer's instructions and gene specific primers used are listed in Table S1. Samples were  
456 loaded onto MicroAmp<sup>®</sup> Optical 384-well reaction plates (Life technologies) in duplicate and run  
457 on the ABI Quant Studio 7 according to manufacturer's instructions. Melting curve analysis was  
458 used to ensure there were no primer dimers. Negative controls included both a no-reverse  
459 transcriptase control and a no cDNA control. Data were analysed by the threshold cycle method  
460 ( $\Delta\Delta$ Ct method)<sup>38</sup> and normalised to *18S* abundance. All data are represented as fold induction  
461 relative to gene expression in uninduced, unstimulated cells or uninfected, unstimulated cells. All  
462 experiments were carried out in triplicate.

#### 463 **Beta-lactamase translocation assay**

464 HeLa cells were seeded in black 96 well trays with transparent well bottom (Greiner Bio-  
465 One) for 16 to 24 h prior to infection. On the day of infection, EPEC strains with derivatives of  
466 pCX340 were cultured as previously described. 2.5 mM Probenecid (Sigma) and 1 mM IPTG

467 (Sigma) were added to bacterial cultures for the last 45 min before infection. HeLa cells were  
468 loaded with CCF2/AM substrate following manufacturer's instructions (Invitrogen) and incubated  
469 at room temperature in the dark for one hour. 15 minutes before infection, cells were transferred  
470 back to 37 °C 5% CO<sub>2</sub>. Infection was carried out using 50 µl of bacterial culture with an OD<sub>600</sub> of  
471 0.1 for 60 min at 37 °C in 5% CO<sub>2</sub>. Translocation was measured as a ratio of  
472 Emission<sub>450nm</sub>:Emission<sub>520nm</sub> using a CLARIOstar Omega microplate reader (BMGLabtech) using  
473 triplicate wells for each strain.

#### 474 **Dual-luciferase reporter assay**

475 For the NF-κB dual-luciferase assay, HeLa cells were seeded into 24-well trays (Corning)  
476 and co-transfected with derivatives of p3xFlag-*Myc*-CMV-24 (0.4 µg), 0.05 µg of pRL-TK  
477 (Promega, Madison WI, USA) and 0.2 µg of pNF-κB-Luc (Clontech, Palo Alto CA, USA).  
478 Approximately 24 h post-transfection, cells were left untreated or stimulated with 20 ng/mL  
479 TNFα (Calbiochem, La Jolla, CA) for 6 h. Firefly and Renilla luciferase levels were measured using  
480 the Dual-luciferase reporter assay system (Promega) in a CLARIOstar Omega microplate reader  
481 (BMGLabtech, Germany). The expression of firefly luciferase was normalised for Renilla luciferase  
482 measurements and Luciferase activity was expressed relative to unstimulated p3xFlag-*Myc*-CMV-  
483 24-transfected cells.

#### 484 ***In vitro* cleavage assays**

485 Purified proteins were diluted out of urea-containing buffer and incubated in 100 µl of  
486 reaction buffer (25 mM NaH<sub>2</sub>PO<sub>4</sub>, 150 mM NaCl, 0.5 mM DTT, pH 7.4) at a concentration of 20  
487 µM (RHIM proteins) or 0.9 µM (EspL/EspL<sub>C47S</sub>) for 1 hour at 37 °C. Sample buffer was then added  
488 to incubated proteins, before the samples were boiled and subjected to SDS-PAGE on Nu-PAGE 4-  
489 12% Bis-Tris polyacrylamide gels. The gels were stained with Coomassie Blue Stain and imaged  
490 with a GelMax imager (UVP, Analytik Jena, USA).

491 To compare the cleavage of RHIM-containing protein in monomeric and fibrillar forms,  
492 10 µg EspL was added to 200 µL of 20 µM of His-Ub-RIPK3 in 25 mM NaH<sub>2</sub>PO<sub>4</sub>, 150 mM NaCl,  
493 0.5 mM DTT, pH 7.4 immediately following dilution of His-Ub-RIPK3 from 8M urea-containing  
494 buffer or after incubation of the diluted His-Ub-RIPK3 for 225 min at 37 °C to allow fibril  
495 formation. Samples were subsequently incubated with EspL at 37 °C for 1 h. For both ‘monomer’  
496 and ‘fibril’ samples, 100 µL was pelleted at 16,000g for 10 min. The supernatant was collected as  
497 the soluble fraction and the pellet was resuspended with 100 µL of 8M urea, pH 4.0. Samples were  
498 subjected to SDS-PAGE and stained with Coomassie Blue Stain for visualisation and imaging as  
499 above.

#### 500 **Thioflavin-T (ThT) assays**

501  
502 Thioflavin-T (ThT) assays were used to monitor fibril formation. 20µM of recombinant  
503 RHIM containing His-Ub-RIPK3 was incubated in buffer (25 mM NaH<sub>2</sub>PO<sub>4</sub>, 150 mM NaCl, 0.5  
504 mM DTT, pH 7.4, 40 µM ThT) in a Costar 96-well plate (Corning) at 37 °C for 3.75 hours inside a  
505 POLARstar Omega microplate reader (BMGLabtech). Samples were excited at 440 nm and ThT  
506 fluorescence emission was measured at 480 nm every 60 seconds. Fibril formation was evident after  
507 225 min. To test the cleavage of RHIM fibrils by EspL, 500 µl of 20 µM of His-Ub-RIPK3 was  
508 dialysed against 1 L of dialysis buffer (25 mM NaH<sub>2</sub>PO<sub>4</sub>, 150 mM NaCl, 0.5 mM DTT, pH 7.4) for  
509 24 h at room temperature. 100 µl of ‘fibril’ sample was then incubated with 0.9 µM purified EspL,  
510 vortexed briefly and incubated at 37 °C for either 1 or 2 h. For both ‘monomer’ and ‘fibril’ samples,  
511 100 µl was pelleted at 16,000 g for 10 min. The supernatant was collected as the soluble fraction  
512 and the pellet was resuspended with 100 µl of 8M urea, pH 4.0. Samples were subjected to SDS-  
513 PAGE and stained with Coomassie Blue Stain for visualisation and imaging as previously  
514 mentioned.

515

516

517 **Reverse-phase HPLC**

518 200–1000  $\mu\text{L}$  of purified RHIM proteins at a concentration of 20  $\mu\text{M}$  were incubated with or  
519 without 0.9  $\mu\text{M}$  of purified EspL for 1 hour at 37 °C. Proteins were then analysed by RP-HPLC  
520 using a C<sub>8</sub> VYDAC column running in MilliQ water containing 0.1% TFA, 10% methanol and  
521 eluted with an increasing gradient of acetonitrile. Peaks were collected and lyophilized for further  
522 analysis by N-terminal sequencing or LC-MS/MS.

523 **N-terminal sequencing**

524 N-terminal sequencing was performed by the Australian Proteome Analysis Facility (APAF)  
525 at Macquarie University, New South Wales, Australia.

526 **Characterisation of His<sub>6</sub>-Ub-RIPK3 and His<sub>6</sub>-Ub-TRIF cleavage products by intact mass**  
527 **spectrometry analysis**

528 Characterisation of RIPK3 and TRIF cleavage products by intact mass spectrometry were  
529 performed on samples prepared by *in vitro* cleavage assay and purified by RP-HPLC as described  
530 above.

531 *Time-of-flight tandem mass spectrometry*

532 Mass measurements of the intact protein ions and ETD and CID MS/MS were performed on the  
533 high resolution, high mass accuracy quadrupole time-of-flight (qTOF) mass spectrometer (maXis II  
534 UHR qTOF, Bruker Daltonics, Bremen, Germany) equipped with an electrospray ion (ESI) source  
535 for the direct-infusion method. For the direct-infusion experiments a flow rate of 180  $\mu\text{L}/\text{min}$  was  
536 provided by a syringe pump (KdScientific, Holliston, MA, USA) using a 25  $\mu\text{L}$  syringe (SGE  
537 Analytical Sciences, VIC, AUS). The following settings were applied: capillary voltage of 4.5 kV,  
538 end plate offset of 500 V, mass range of  $m/z$  450 to 2500, dry gas of 4.0 L/min, and drying  
539 temperature of 220 °C. Nano-ESI infusion was performed using HPLC fractions which were  
540 reconstituted in 20  $\mu\text{L}$  of water and diluted 1:10 with 50% acetonitrile: 50% water containing 1%  
541 formic acid.

542 *Data analysis*

543 The MS and MS/MS spectra were analyzed using a dedicated top-down data analysis procedure.  
544 Briefly, precursor and product ion mass spectra were summed over the infusion time in each MS  
545 and MS/MS experiment with Data Analysis software version 4.3 (Bruker Daltonics). Automatic  
546 data analysis was performed by deisotoping keeping only the monoisotopic masses followed by  
547 charge state deconvolution (SNAP 2 algorithm). The obtained mass list of product ions was  
548 matched on the predicted cleaved mRIPK3 sequence to determine the product ion identity and the  
549 sequence coverage using the observed mass of the precursor ion.

550 **Necroptosis experiments.** The human epithelial cell line, HT-29, as well as mouse dermal  
551 fibroblasts (MDF) and immortalised bone marrow derived macrophages (iBMDMs) either infected  
552 with derivatives of EPEC E2348/69 or engineered to express EspL derivatives were used to  
553 examine the effect of EspL on necroptosis. Necroptosis was induced by treatment with 1) 20 ng/mL  
554 TNF, 500 nM Cp.A and 25  $\mu$ M z-VAD-FMK or 50  $\mu$ M QVD-OPH or 2) 20 ng/mL of LPS (*E. coli*  
555 0111:B4) and 10  $\mu$ M z-VAD-FMK or 3) 50  $\mu$ g/mL Poly I:C (for iBMDMs) or 10  $\mu$ g/mL high  
556 molecular weight Poly I:C (for HT-29) and 10  $\mu$ M z-VAD-FMK. Cell viability was assessed by  
557 reduction of 3-(4,5-Dimethylthiazol-2-yl)-2,5- diphenyltetrazolium bromide (MTT) or by  
558 propidium iodide (PI) uptake. MLKL complex formation and membrane translocation were  
559 examined by Blue native PAGE of cell membrane and cytosolic fractions and immunoblotting  
560 using antibodies to MLKL and phospho-MLKL.

561 **Protein sequence alignment and phylogenetic tree**

562 RHIM domain alignment for human and mouse RIPK1, RIPK3, TRIF and DAI was  
563 performed by Clustal Omega and ESPript<sup>39</sup>. Accession numbers (same order as displayed in Fig.  
564 2c) NP\_003795, NP\_033094, NP\_006862, NP\_064339, NP\_891549, NP\_778154, NP\_110403,  
565 NP\_067369, NP\_001153889, NP\_001132991. For comparison of the cysteine protease motif,  
566 sequences were identified through BLAST using EspL from EPEC E2348/69 as a reference. A



567 section of the proteins identified by BLAST were aligned using Clustal Omega and presentation of  
568 alignment performed using ESPript3<sup>39</sup>. Accession numbers (same order as displayed in  
569 Supplementary Figure Fig. 2) CAS10778, AIG70345, WP\_012905388, WP\_031942474,  
570 WP\_024259347, ENZ84489, WP\_023263817, WP\_015872003, WP\_020957625, CCA83579,  
571 WP\_009667375, CDG86051, WP\_004389152, WP\_004714204, WP\_019080404, AHK18540,  
572 WP\_002211641, AIN16488.

573 A set of protein sequences was curated based on the identification of homologues of EspL  
574 from EPEC E2348/69. BLAST<sup>25</sup> was used to compare these protein sequences to the *nr* database  
575 and *nt* database (downloaded on 31<sup>st</sup> July from <ftp://ftp.ebi.edu.au/pub/databases/ncbi/blast/db/>)  
576 with blastp and tblastn respectively to identify additional proteins. The subsequent results were  
577 filtered on the E scores of 0.0 and length, and reduced to unique accession (removing duplicates).  
578 The nucleotide sequences were translated into amino acid sequences with EMBOSS<sup>40</sup> and the  
579 protein sequences were aligned with Muscle<sup>41</sup>. The best fitting protein model was determined using  
580 the Perl script ProteinModelSelection.pl available at <http://sco.hits.org/exelixis/web/software/raxml/>  
581 for RAxML<sup>42</sup>. One hundred pseudo-replicate RAxML analyses were run three times using the best-  
582 fitting substitution model, PROTGAMMA VF. The best scoring Maximum Likelihood tree was  
583 selected and midpoint rooted in Dendroscope<sup>43</sup>. The following accession numbers were used for  
584 phylogenetic analyses; CAS10778.1, AIG70345.1, CBG87854.1, ACR69900, CP001064,  
585 CP011417, LM996972, LM997319, CP001064, Z54194, WP\_028120439, LM996116,  
586 WP\_028120664, WP\_038348374, AJ303141 LM996576, AP010958, LM995478, LM995537,  
587 LM996653, LM997233, LM997407, LM995613, LM997087, WP\_001121612, WP\_001121619,  
588 WP\_001121621, WP\_033810450, WP\_044863368, AAJV00000000, AIAN00000000, FM986650,  
589 AP010960, LM996367, EHW09036, EHW21689, WP\_001121623, WP\_001121627,  
590 WP\_001121746, WP\_001121747, WP\_001121748, WP\_021824236, WP\_023981847,  
591 WP\_032272532, WP\_032273780, AIHA00000000, WP\_032349748, AIHB00000000,

592 AIHD00000000, AIHE00000000, AAJX00000000, AIBC00000000, LN554915, LM996042,  
593 LM996071, LM996922, WP\_001121620, WP\_032210130, AKNI01000047, AIAL00000000,  
594 AIAO00000000, AIGY00000000, AIGZ00000000, AIBX00000000, CP006262, CP007133,  
595 LM996313, LM996458, CP007136, LM995993, LM996803, LM997001, WP\_001121622,  
596 AIAI00000000, AIAX00000000, AF453441, AIBD00000000, CP008805, CP001164, CP001368,  
597 CP001925, CP010304, EHV10408, WP\_001121626, WP\_024256897, WP\_032208682,  
598 AIAQ00000000, LM995690, LM995751, LM995947, AJ277443, FM201463, LM995831,  
599 LM996694, LM997125, EHW62569, WP\_001121617, WP\_032345473, WP\_045889142,  
600 AICF00000000, AIAC00000000, AIGK00000000, AIGN00000000, AIGO00000000,  
601 AIAG00000000, AIGL00000000, AIGM00000000, AIBT00000000, AIBR00000000,  
602 AIBV00000000, AIGX00000000, WP\_001121628, CP001846, CP003109, WP\_001121608,  
603 WP\_001121609, WP\_001121624, AIAH00000000, AIAD00000000, ADUL01000000,  
604 AIFD00000000, AIAE00000000, AIFS00000000, AIFT00000000, AIFU00000000,  
605 AIFQ00000000, FM986652, LM996749, CDG86051, WP\_038497945, WP\_009667375,  
606 CCA83579, FP885907, AEG72234, CBJ36034, CEJ16658, EUJ11993, WP\_003265371,  
607 WP\_003274329, WP\_013209029, WP\_039553678, WP\_042549988, WP\_042592182,  
608 WP\_043947056, ENZ84489, CP000037, CP001062, WP\_012421777, CP000035, CP006737,  
609 ADA76828, EFP73031, EFW48342, WP\_000608472, WP\_005015229, WP\_011379052,  
610 AY879342, NG\_035859, NG\_035867, AF348706, AF386526, AL391753, AY879342, CP001384,  
611 CP007038, Z54211, CAA90938, EIQ30821, WP\_005058548, WP\_005061014, WP\_005065444,  
612 WP\_005115993, WP\_005117432, WP\_010921597, WP\_010921642, WP\_015060143,  
613 WP\_024259347, WP\_025746267, WP\_025748914, WP\_025759433, WP\_025766126,  
614 WP\_031942474, WP\_039060413, WP\_040234710, WP\_047204882, WP\_047204897, CP000039,  
615 CP011423, HE616529, WP\_005041841, WP\_005138925, WP\_024261348, CFB70006,  
616 CFQ67145, CNC44257, CRE36360, WP\_019080404, CFR06093, WP\_004389152, CP000305,

617 CP001585, CP001589, CP001608, CP002956, CP009492, CP009704, CP009723, CP009785,  
618 CP009836, CP009844, CP009973, CP009996, CP010023, CP010293, AE009952, AE017042,  
619 AL590842, CP000308, CP001593, CP009840, CP009906, CP009991, KGA51839,  
620 WP\_002211641, WP\_045123609, BX936398, CP001048, CP009757, CP009780, CP009786,  
621 CP010067, CP000950, CP008943, CP009712, CP009759, CP009792, CFV36814, CNG55237,  
622 CNJ16181, WP\_011193035, WP\_012104544, WP\_012303595, ESJ22116.1, WP\_032466541,  
623 WP\_038400874, WP\_004714204, CP007230, CNC46702, WP\_025381344, WP\_006576111.1

#### 624 **Mouse infection studies**

625 All animal experimentation was approved by the Melbourne University Animal Ethics  
626 Committee. All mice used were of a C57BL/6 background and were age matched as best as possible  
627 between 5-8 weeks pre-infection. No calculation was used to assess the number of animals required.  
628 Male and female mice were allocated to experimental groups to ensure even distribution of age, sex  
629 and weight and investigators were not blinded to the allocation. *Citrobacter rodentium* was cultured  
630 in LB broth overnight before centrifugation and re-suspension in PBS to a concentration of  $\sim 5 \times 10^9$   
631 cells/mL. C57BL/6 (5- to 8 weeks old) were inoculated by oral gavage with 200  $\mu$ l of  
632 approximately  $1 \times 10^9$  c.f.u of *C. rodentium*. The viable count of the inoculum was determined  
633 retrospectively by plating dilutions of the inoculum on plates with appropriate antibiotics. Mice  
634 were weighed every 2 days and faeces collected every 2 or 4 days for enumeration of c.f.u. The  
635 viable count per g of faeces was determined by plating serial dilutions of faeces onto media  
636 containing selective antibiotics.

637 **Statistical analysis.** All statistical analyses were performed using GraphPad Prism version 6.0.  
638 Statistical tests used were unpaired two-tailed Student's *t*-test for pairwise comparisons between  
639 groups or One-way ANOVA with Holm-Sidak's Test for multiple comparisons where indicated.  
640 Variance was similar in all comparisons. Differences in faecal counts of CR from mice and

641 diarrhoea and pathology scores were assessed using a Mann Whitney U test, where normal  
642 distribution was not assumed.  $P < 0.05$  was considered to be significant.

643 **Data availability.** The data that support the findings of this study are available from the  
644 corresponding author upon request

645

647 **References**

- 648 1 Sun, X., Yin, J., Starovasnik, M. A., Fairbrother, W. J. & Dixit, V. M. Identification of a  
649 novel homotypic interaction motif required for the phosphorylation of receptor-interacting  
650 protein (RIP) by RIP3. *J Biol Chem* **277**, 9505-9511 (2002).
- 651 2 Kaiser, W. J. & Offermann, M. K. Apoptosis induced by the toll-like receptor adaptor TRIF  
652 is dependent on its receptor interacting protein homotypic interaction motif. *J Immunol* **174**,  
653 4942-4952 (2005).
- 654 3 Rebsamen, M. *et al.* DAI/ZBP1 recruits RIP1 and RIP3 through RIP homotypic interaction  
655 motifs to activate NF-kappaB. *EMBO Rep* **10**, 916-922 (2009).
- 656 4 Li, J. *et al.* The RIP1/RIP3 necrosome forms a functional amyloid signaling complex  
657 required for programmed necrosis. *Cell* **150**, 339-350 (2012).
- 658 5 Pasparakis, M. & Vandenabeele, P. Necroptosis and its role in inflammation. *Nature* **517**,  
659 311-320 (2015).
- 660 6 Micheau, O. & Tschopp, J. Induction of TNF receptor I-mediated apoptosis via two  
661 sequential signaling complexes. *Cell* **114**, 181-190 (2003).
- 662 7 Holler, N. *et al.* Fas triggers an alternative, caspase-8-independent cell death pathway using  
663 the kinase RIP as effector molecule. *Nat Immunol* **1**, 489-495 (2000).
- 664 8 Cho, Y. S. *et al.* Phosphorylation-driven assembly of the RIP1-RIP3 complex regulates  
665 programmed necrosis and virus-induced inflammation. *Cell* **137**, 1112-1123 (2009).
- 666 9 He, S. *et al.* Receptor interacting protein kinase-3 determines cellular necrotic response to  
667 TNF-alpha. *Cell* **137**, 1100-1111 (2009).
- 668 10 Murphy, J. M. *et al.* The pseudokinase MLKL mediates necroptosis via a molecular switch  
669 mechanism. *Immunity* **39**, 443-453 (2013).
- 670 11 Sun, L. *et al.* Mixed lineage kinase domain-like protein mediates necrosis signaling  
671 downstream of RIP3 kinase. *Cell* **148**, 213-227 (2012).
- 672 12 Cai, Z. *et al.* Plasma membrane translocation of trimerized MLKL protein is required for  
673 TNF-induced necroptosis. *Nat Cell Biol* **16**, 55-65 (2014).
- 674 13 Hildebrand, J. M. *et al.* Activation of the pseudokinase MLKL unleashes the four-helix  
675 bundle domain to induce membrane localization and necroptotic cell death. *Proc Natl Acad*  
676 *Sci U S A* **111**, 15072-15077 (2014).
- 677 14 Kaiser, W. J. *et al.* Toll-like receptor 3-mediated necrosis via TRIF, RIP3, and MLKL. *J*  
678 *Biol Chem* **288**, 31268-31279 (2013).
- 679 15 Upton, J. W., Kaiser, W. J. & Mocarski, E. S. DAI/ZBP1/DLM-1 complexes with RIP3 to  
680 mediate virus-induced programmed necrosis that is targeted by murine cytomegalovirus  
681 vIRA. *Cell Host Microbe* **11**, 290-297 (2012).
- 682 16 Lawlor, K. E. *et al.* RIPK3 promotes cell death and NLRP3 inflammasome activation in the  
683 absence of MLKL. *Nat Commun* **6**, 6282 (2015).
- 684 17 Giogha, C., Lung, T. W., Pearson, J. S. & Hartland, E. L. Inhibition of death receptor  
685 signaling by bacterial gut pathogens. *Cytokine Growth Factor Rev* **25**, 235-243 (2014).
- 686 18 Pearson, J. S. *et al.* A type III effector antagonizes death receptor signalling during bacterial  
687 gut infection. *Nature* **501**, 247-251 (2013).
- 688 19 Li, S. *et al.* Pathogen blocks host death receptor signalling by arginine GlcNAcylation of  
689 death domains. *Nature* **501**, 242-246 (2013).
- 690 20 Zhang, L. *et al.* Cysteine methylation disrupts ubiquitin-chain sensing in NF-kappaB  
691 activation. *Nature* **481**, 204-208 (2012).

- 692 21 Charpentier, X. & Oswald, E. Identification of the secretion and translocation domain of the  
693 enteropathogenic and enterohemorrhagic *Escherichia coli* effector Cif, using TEM-1 beta-  
694 lactamase as a new fluorescence-based reporter. *J Bacteriol* **186**, 5486-5495 (2004).
- 695 22 Wertz, I. E. *et al.* De-ubiquitination and ubiquitin ligase domains of A20 downregulate NF-  
696 kappaB signalling. *Nature* **430**, 694-699 (2004).
- 697 23 Newton, K. *et al.* Ubiquitin chain editing revealed by polyubiquitin linkage-specific  
698 antibodies. *Cell* **134**, 668-678 (2008).
- 699 24 Lin, Y., Devin, A., Rodriguez, Y. & Liu, Z. G. Cleavage of the death domain kinase RIP by  
700 caspase-8 prompts TNF-induced apoptosis. *Genes Dev* **13**, 2514-2526 (1999).
- 701 25 Altschul, S. F., Gish, W., Miller, W., Myers, E. W. & Lipman, D. J. Basic local alignment  
702 search tool. *J Mol Biol* **215**, 403-410 (1990).
- 703 26 Kelley, L. A. & Sternberg, M. J. Protein structure prediction on the Web: a case study using  
704 the Phyre server. *Nat Protoc* **4**, 363-371 (2009).
- 705 27 Shao, F., Merritt, P. M., Bao, Z., Innes, R. W. & Dixon, J. E. A *Yersinia* effector and a  
706 *Pseudomonas* avirulence protein define a family of cysteine proteases functioning in  
707 bacterial pathogenesis. *Cell* **109**, 575-588 (2002).
- 708 28 Humphries, F., Yang, S., Wang, B. & Moynagh, P. N. RIP kinases: key decision makers in  
709 cell death and innate immunity. *Cell Death Differ* **22**, 225-236 (2015).
- 710 29 Vince, J. E. *et al.* IAP antagonists target cIAP1 to induce TNFalpha-dependent apoptosis.  
711 *Cell* **131**, 682-693 (2007).
- 712 30 Wickham, M. E. *et al.* Bacterial genetic determinants of non-O157 STEC outbreaks and  
713 hemolytic-uremic syndrome after infection. *J Infect Dis* **194**, 819-827 (2006).
- 714 31 Conzen, S. D. & Cole, C. N. The three transforming regions of SV40 T antigen are required  
715 for immortalization of primary mouse embryo fibroblasts. *Oncogene* **11**, 2295-2302 (1995).
- 716 32 Hornung, V. *et al.* Silica crystals and aluminum salts activate the NALP3 inflammasome  
717 through phagosomal destabilization. *Nat Immunol* **9**, 847-856 (2008).
- 718 33 Tanzer, M. C. *et al.* Evolutionary divergence of the necroptosis effector MLKL. *Cell Death*  
719 *Differ* **23**, 1185-1197 (2016).
- 720 34 Catanzariti, A. M., Soboleva, T. A., Jans, D. A., Board, P. G. & Baker, R. T. An efficient  
721 system for high-level expression and easy purification of authentic recombinant proteins.  
722 *Protein Sci* **13**, 1331-1339 (2004).
- 723 35 Galan, J. E., Ginocchio, C. & Costeas, P. Molecular and functional characterization of the  
724 Salmonella invasion gene invA: homology of InvA to members of a new protein family. *J*  
725 *Bacteriol* **174**, 4338-4349 (1992).
- 726 36 Datsenko, K. A. & Wanner, B. L. One-step inactivation of chromosomal genes in  
727 *Escherichia coli* K-12 using PCR products. *Proc Natl Acad Sci U S A* **97**, 6640-6645.  
728 (2000).
- 729 37 McKenzie, G. J. & Craig, N. L. Fast, easy and efficient: site-specific insertion of transgenes  
730 into enterobacterial chromosomes using Tn7 without need for selection of the insertion  
731 event. *BMC Microbiol* **6**, 39 (2006).
- 732 38 Huang, K. F., Chiou, S. H., Ko, T. P., Yuann, J. M. & Wang, A. H. The 1.35 A structure of  
733 cadmium-substituted TM-3, a snake-venom metalloproteinase from Taiwan habu:  
734 elucidation of a TNFalpha-converting enzyme-like active-site structure with a distorted  
735 octahedral geometry of cadmium. *Acta Crystallogr D Biol Crystallogr* **58**, 1118-1128  
736 (2002).
- 737 39 Gouet, P., Courcelle, E., Stuart, D. I. & Metz, F. ESPript: analysis of multiple sequence  
738 alignments in PostScript. *Bioinformatics* **15**, 305-308 (1999).
- 739 40 Coppolino, M. G. *et al.* Requirement for N-ethylmaleimide-sensitive factor activity at  
740 different stages of bacterial invasion and phagocytosis. *J Biol Chem* **276**, 4772-4780 (2001)

741 41 Edgar, R. C. MUSCLE: a multiple sequence alignment method with reduced time and space  
742 complexity. *BMC Bioinformatics* **5**, 113 (2004).

743 42 Stamatakis, A. RAxML version 8: a tool for phylogenetic analysis and post-analysis of large  
744 phylogenies. *Bioinformatics* **30**, 1312-1313 (2014).

745 43 Huson, D. H. & Scornavacca, C. Dendroscope 3: an interactive tool for rooted phylogenetic  
746 trees and networks. *Syst Biol* **61**, 1061-1067 (2012).

747 44 Levine, M. M. *et al.* Escherichia coli strains that cause diarrhoea but do not produce heat-  
748 labile or heat-stable enterotoxins and are non-invasive. *Lancet* **1**, 1119-1122 (1978).

749 45 Newton, H. J. *et al.* The type III effectors NleE and NleB from enteropathogenic *E. coli* and  
750 OspZ from *Shigella* block nuclear translocation of NF-kappaB p65. *PLoS Pathog* **6**,  
751 e1000898 (2010).

752 46 Garmendia, J. *et al.* TccP is an enterohaemorrhagic *Escherichia coli* O157:H7 type III  
753 effector protein that couples Tir to the actin-cytoskeleton. *Cell Microbiol* **6**, 1167-1183  
754 (2004).

755 47 Mundy, R. *et al.* Identification of a novel type IV pilus gene cluster required for  
756 gastrointestinal colonization of *Citrobacter rodentium*. *Mol Microbiol* **48**, 795-809 (2003).

757 48 Kelly, M. *et al.* Essential role of the type III secretion system effector NleB in colonization  
758 of mice by *Citrobacter rodentium*. *Infect Immun* **74**, 2328-2337 (2006).

759 49 Yamamoto, M. *et al.* A cluster of interferon-gamma-inducible p65 GTPases plays a critical  
760 role in host defense against *Toxoplasma gondii*. *Immunity* **37**, 302-313 (2012)

761

762

763

764 **Legend to the figures**

765 **Figure 1. EspL is a T3SS cysteine protease that degrades RIPK1 and RIPK3. a,** Schematic

766 representation of EPEC E2348/69 genomic integrative element 6 (IE6) harbouring *espL*, *nleB1*, and

767 *nleE* and immunoblot showing RIPK1 degradation in HT-29 cells infected with derivatives of

768 EPEC E2348/69 as shown. Representative immunoblot from at least 3 independent experiments.

769 Actin; loading control. **b,** Immunoblot showing RIPK1 degradation in HeLa cells uninfected or

770 infected with EPEC E2348/69; untreated, or treated with either MG132 or z-VAD-FMK (z-VAD).

771 Representative immunoblot from at least three independent experiments. Actin; loading control. **c,**

772 Schematic representation of cysteine protease motif and secondary structure predicted by Phyre in

773 YopT from *Y. pestis* KIM and EspL from EPEC E2348/69. **d,** Immunoblot showing levels of

774 RIPK1, RIPK2 and RIPK3 in HT-29 cells infected with derivatives of EPEC E2348/69.

775 Representative immunoblot from at least three independent experiments. Actin; loading control.

776

777 **Figure 2. Distribution of EspL in Gram negative pathogens and substrate specificity. a,**

778 Phylogeny of EspL homologues from a range of Gram negative pathogens which was midpoint

779 rooted. Different genera are highlighted by background colour and the tips are coloured by species

780 or pathotype. **b,** Coomassie Brilliant Blue stain of SDS PAGE gel showing *in vitro* cleavage of

781 purified RHIM-containing regions of RIPK1, RIPK3, TRIF and ZBP1 (expressed as recombinant

782 His<sub>6</sub>-ubiquitin-tagged proteins) by purified recombinant EspL. Representative gel from at least two

783 independent experiments. Purified recombinant EspL<sub>C47S</sub> was used as a negative control. White

784 arrows indicate cleavage products. Black arrows indicate EspL and the band corresponding to free

785 His<sub>6</sub>-ubiquitin (His-Ub) Note, observed cleavage product derived from ZBP1/DAI was consistent

786 with EspL cleavage in first RHIM of ZBP1/DAI. **c,** EspL cleavage site indicated by an arrow in the

787 RHIM containing regions of RIPK1, RIPK3, TRIF and ZBP1/DAI. Alignment was performed using



788 Clustal Omega and ESPript3. Cleavage sites in RIPK3 and TRIF were determined experimentally  
789 by mass spectrometry and N-terminal sequencing.

790

791 **Figure 3. EspL inhibits TNF-induced necroptosis. a,** Cell death visualised by propidium iodide  
792 (PI) staining in HT-29 cells infected with derivatives of EPEC and treated with TNF, compound A  
793 (Cp.A) and z-VAD-FMK (z-VAD). Hoechst; stain for nucleic acid. Scale bar, 20  $\mu$ m.  
794 Representative images shown from at least three independent experiments. **b,** Quantification of PI  
795 staining from microscopic analysis in HT-29 cells infected with derivatives of EPEC E2348/69 and  
796 treated with TNF, Cp.A and z-VAD. Results are mean  $\pm$  s.e.m. percentage of cells positive for PI  
797 staining from three independent experiments counting  $\sim$ 200 cells in triplicate. \* $P$ <0.0001 compared  
798 to EPEC E2348/69 infected cells, one-way ANOVA with Holm-Sidak multiple comparison. **c,** Blue  
799 native PAGE analysis of MLKL membrane translocation in HT-29 cells infected with derivatives of  
800 EPEC E2348/69 treated with TNF, Cp.A and z-VAD. Representative immunoblot from at least  
801 three independent experiments. GAPDH; cytosolic fraction loading control, VDAC; membrane  
802 fraction loading control.

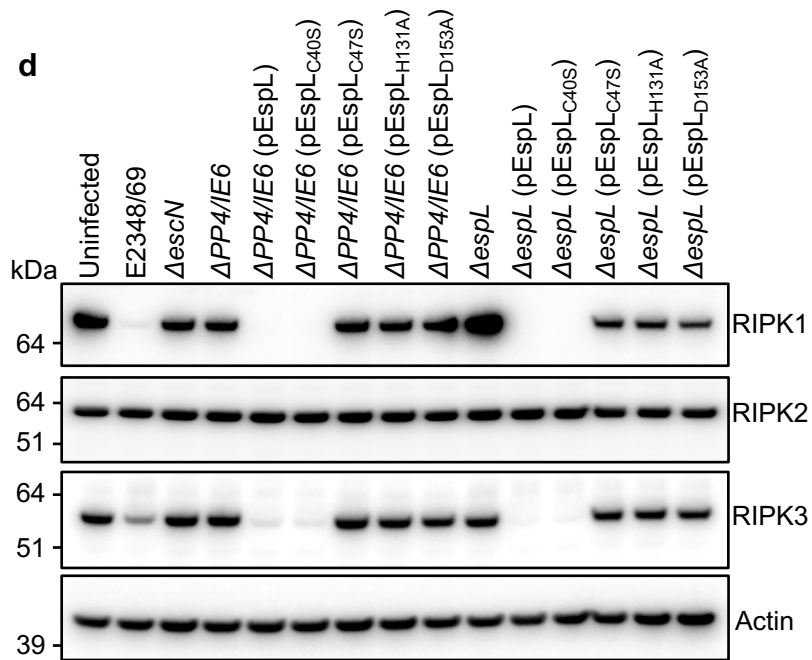
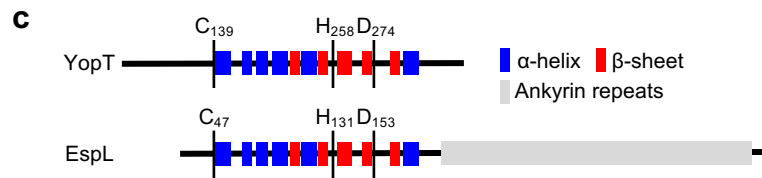
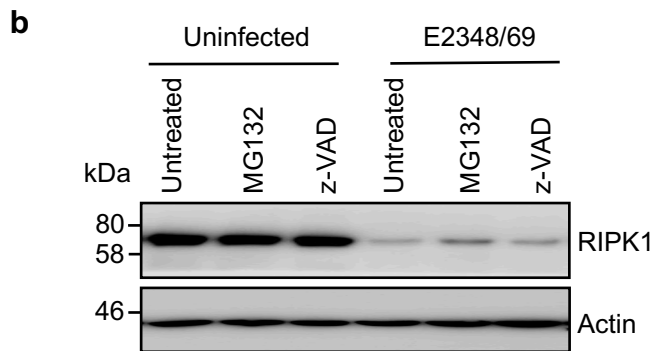
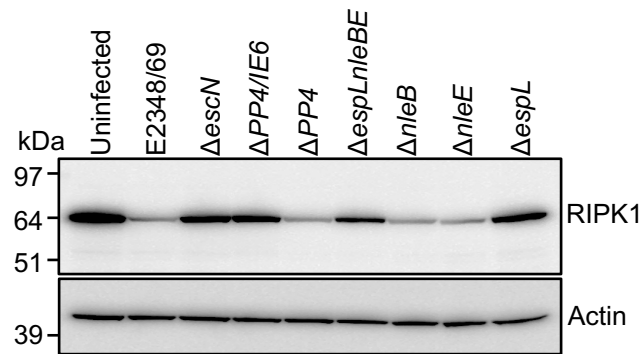
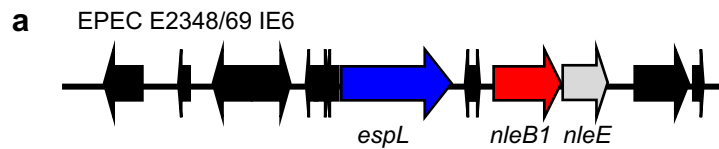
803

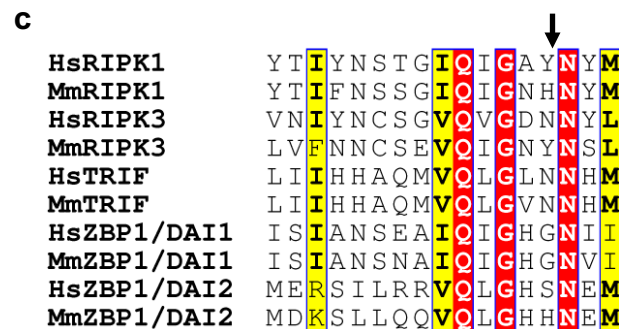
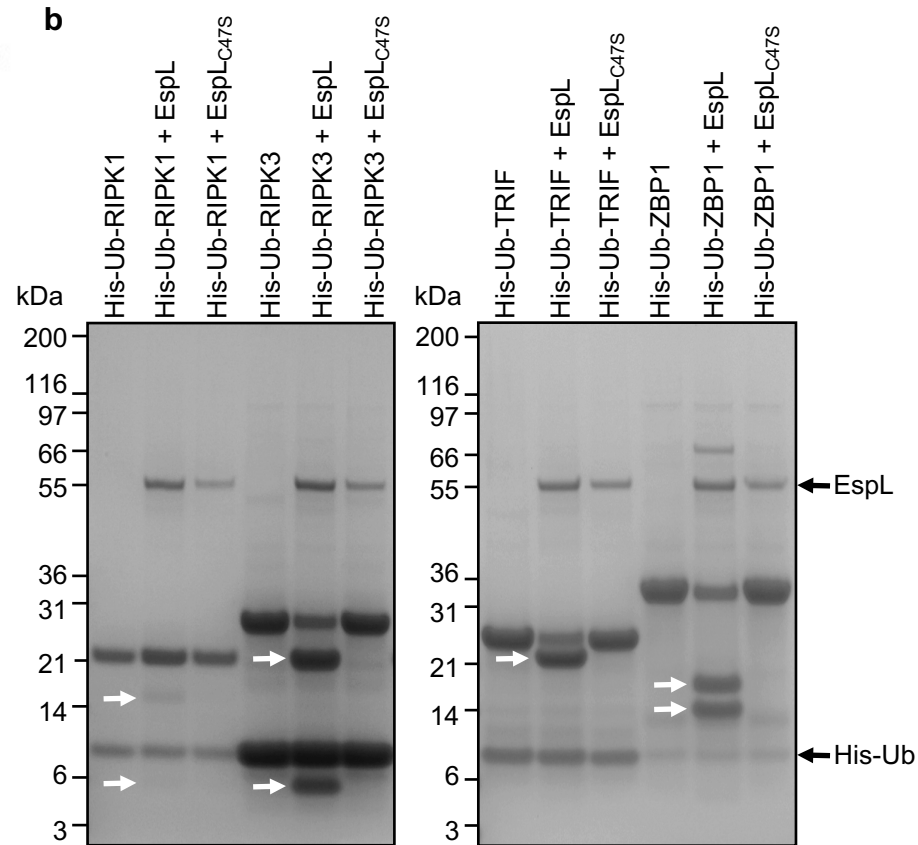
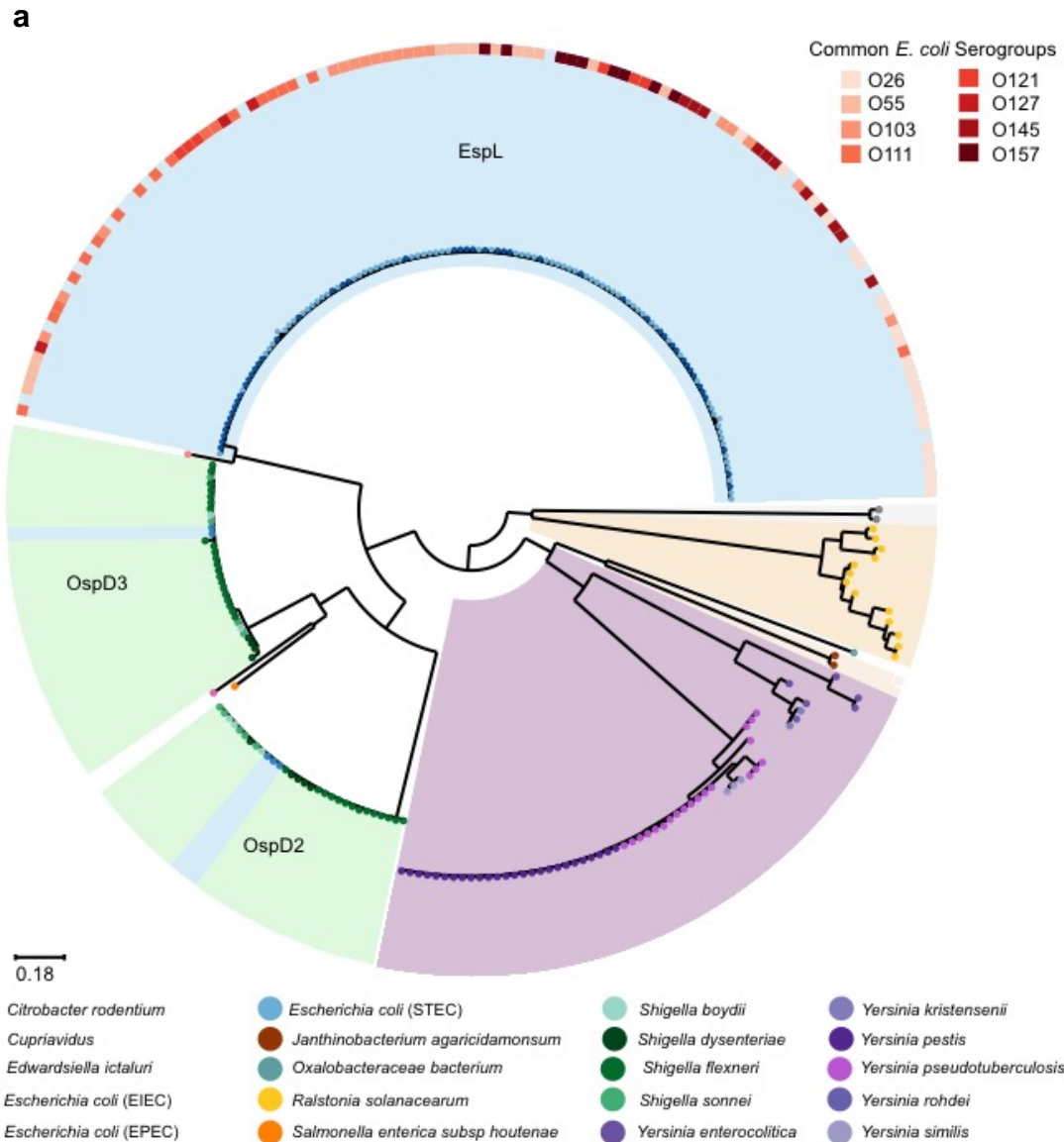
804 **Figure 4. EspL activity inhibits TLR3/4-mediated signalling and contributes to *in vivo***  
805 **persistence. a,** *Ifn $\beta$*  expression in doxycycline-inducible iBMDMs stably expressing either Flag-  
806 EspL or Flag-EspL<sub>C47S</sub> and treated with either LPS or Poly I:C for 3 h as indicated. Results are mean  
807  $\pm$  s.e.m of at least three independent experiments performed in triplicate. *Ifn $\beta$*  expression relative to  
808 uninduced, unstimulated cells. \* $P$ <0.0005 compared to Flag-EspL induced with doxycycline and  
809 treated with LPS or poly I:C, unpaired, two-tailed *t*-test. **b,** MTT reduction in doxycycline-inducible  
810 iBMDMs stably expressing either Flag-EspL or Flag-EspL<sub>C47S</sub> and treated with either LPS/z-VAD  
811 or Poly I:C/z-VAD for 20 h. Results are mean  $\pm$  s.e.m. of absorbance at 540 nm from three  
812 independent experiments performed in triplicate. \* $P$ < 0.05 compared to Flag-EspL<sub>C47S</sub> induced with

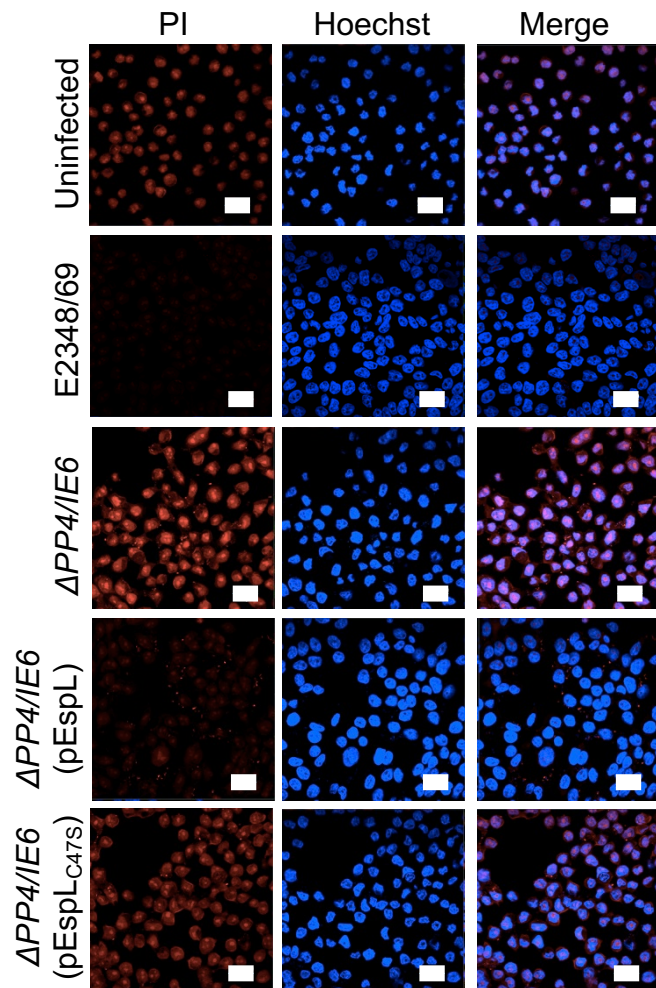
813 doxycycline and treated with LPS or poly I:C, unpaired, two-tailed *t*-test. **c**, Immunoblot showing  
814 degradation of endogenous RIPK1 by EspL from *C. rodentium* (Flag-CREspL) but not EspL<sub>C42S</sub>  
815 (Flag-CREspL<sub>C42S</sub>) expressed ectopically in HEK293T cells. Representative immunoblot from at  
816 least three independent experiments. **d**, Bacterial load in the faeces of mice 16 days after infection  
817 with derivatives of *C. rodentium*, including wild type *C. rodentium* ICC169 (CR), an *espL* deletion  
818 mutant ( $\Delta espL$ ) and  $\Delta espL$  complemented with *espL* (EspL) or *espL*<sub>C42S</sub> (EspL<sub>C42S</sub>) by Tn7  
819 transposition. Each data point represents log<sub>10</sub> c.f.u. per g faeces per individual animal (c.f.u.,  
820 colony forming units). Mean  $\pm$  s.e.m. are indicated. Data was combined from three independent  
821 experiments. *P* values from Mann–Whitney U-test.

822

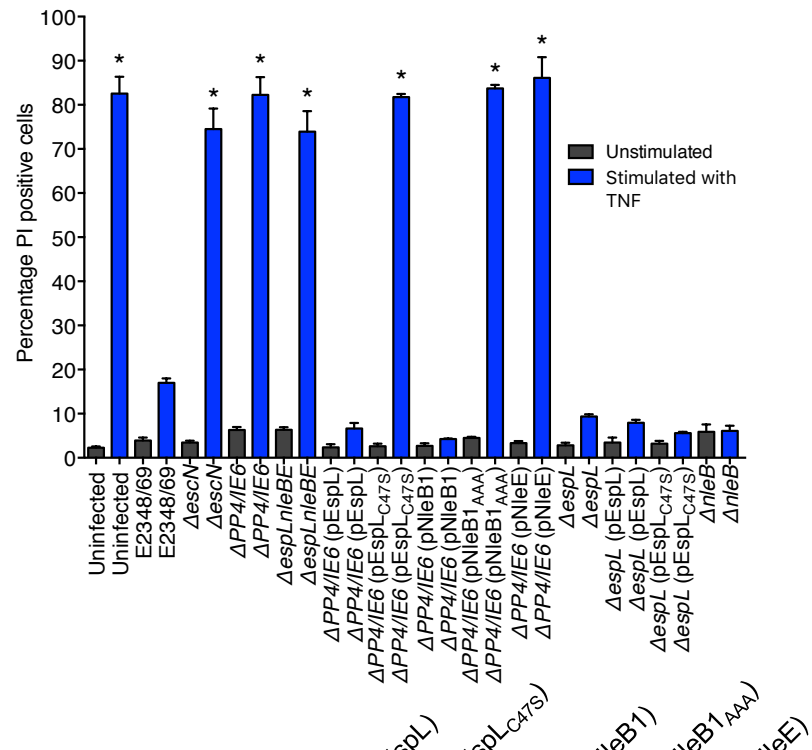
823





**a**

+ TNF/Cp.A/z-VAD

**b****c**